



Modeling and simulation of photovoltaic (PV) system during partial shading based on a two-diode model

Kashif Ishaque^a, Zainal Salam^{a,*}, Hamed Taheri^a, Syfaruddin^b

^a Faculty of Electrical Engineering, Universiti Teknologi Malaysia, UTM 81310, Skudai, Johor Bahru, Malaysia

^b Kumamoto University, 2-39-1 Kurokami, Kumamoto 860-8555, Japan

ARTICLE INFO

Article history:

Received 17 August 2010

Received in revised form 6 April 2011

Accepted 11 April 2011

Available online 7 May 2011

Keywords:

PV module

Partial shading

Two-diode model

Local maxima

Global maxima

ABSTRACT

This paper proposes accurate partial shading modeling of photovoltaic (PV) system. The main contribution of this work is the utilization of the two-diode model to represent the PV cell. This model requires only four parameters and known to have better accuracy at low irradiance level, allowing for more accurate prediction of PV system performance during partial shading condition. The proposed model supports a large array simulation that can be interfaced with MPPT algorithms and power electronic converters. The accurateness of the modeling technique is validated by real time simulator data and compared with the three other types of modeling, namely Neural Network, P&O and single-diode model. It is envisaged that the proposed work is very useful for PV professionals who require simple, fast and accurate PV model to design their systems.

© 2011 Published by Elsevier B.V.

1. Introduction

Photovoltaic (PV) power system is envisaged to become an important renewable energy source due to its pollution-free and inexhaustible nature. Large scale PV power systems have been commercialized in numerous countries due to their substantial long term benefits, generous feed-in tariff schemes and other initiatives provided by governments to promote sustainable green energy. However, due to the high investment cost on PV modules, optimal utilization of the available solar energy has to be ensured. This necessitates a precise and reliable simulation of the designed PV systems prior to installation.

The most important component that affects the accuracy of the simulation is the PV cell model. Modeling of PV cell involves the estimation of the I - V and P - V characteristics curves to emulate the real cell under various environmental conditions. The most popular approach is to utilize the electrical equivalent circuit, which is primarily based on diode. Many models have been proposed by various researchers; the simplest is the basic single-diode model. It comprises of a linear independent current source in parallel to a diode [1–4]. The model only requires three parameters to completely characterize the I - V curve, namely short-circuit current (I_{sc}), open circuit voltage (V_{oc}) and diode ideality factor (a). An improvement of this model is done by the inclusion of one series resistance, R_s [5–10]. In literature, it is popularly known as the R_s -model. Due to its simplicity and computational efficiency, the R_s is by far the most widely used model in PV system simulation [6]. However it exhibits serious deficiencies when subjected to temperature variations; its accuracy is known to deteriorate at high temperature. Further extension of the R_s -model, called as the R_p -model, which includes an additional shunt resistance R_p was introduced [11–15]. Although some improvement is achieved, this model demands significant computing effort because the parameters have been increased to five. Furthermore its accuracy deteriorates at low irradiance, especially in the vicinity of the open circuit voltage, V_{oc} .

* Corresponding author. Tel: +60 7 5536187; fax: +60 7 5566272.

E-mail addresses: kashif@fkegraduate.utm.my (K. Ishaque), zainals@fke.utm.my (Z. Salam).

With the availability of today's vast computing power, more accurate (but complicated) PV models are proposed. One important example is the two-diode model, originally introduced by [16]. The inclusion of the additional diode increases the parameters from five (for R_p -model) to seven. The main challenge now is to estimate the values of all the model parameters while maintaining a reasonable simulation time. The key is to realize an efficient and fast computation method to calculate the values of these parameters.

Several computational methods are proposed [17–20] but in all these techniques, new additional coefficients are introduced into the equations, increasing their computational burdens. Furthermore difficulty arises in determining the initial values of the parameters; in some cases heuristic solutions need to be sought. Another approach to describe the two-diode model is by investigating its physical characteristics such as the electron diffusion coefficient, minority carrier's lifetime, intrinsic carrier density and other semiconductor parameters [21–24]. Whilst these models can be helpful in understanding the physical behavior of the cell, information about the semiconductor is not always available in commercial PV datasheets. Hence a useful simulator using such model is not feasible because in majority of the cases, PV system designers are not equipped with the detail knowledge of the semiconductor processes.

Once the appropriate model and its computational model have been identified, a complete PV system simulation can be developed. A good PV simulation package should fulfill the following criteria: (1) it should be fast but can accurately predict the I - V and P - V characteristic curves; including special conditions such as partial shading (2) it should be a comprehensive tool to develop and validate the PV system design inclusive of the power converter and MPPT control. Although existing software packages like PSpice, PV-DesignPro, SolarPro, PVcad, and PVsyst are available in the market, they are expensive, unnecessarily complex and rarely support the interfacing of the PV arrays with power converters [25].

Over the years, several researchers have studied the characteristics of PV modules under partial shading conditions [26,27]. In [26], an experimental work was undertaken to characterize the I - V curve during partial shading but the scope was limited to module-level shading. In a real PV generation system, a large number of modules are interconnected to form arrays; thus module-level shading would not be effective to investigate the shading phenomena. The effect of shading on the output of the PV modules and the associated change in their I - V characteristics was investigated in [27]. However, the I - V and P - V characteristics do not visualize the occurrence of multiple peaks, which are usually present in the I - V and P - V characteristics when subjected to partial shading. In another work, a numerical algorithm was proposed in [28] to simulate the complex characteristics of a PV array by representing each element (each cell of the module, bypass diode, blocking diode, etc.) with mathematical expressions. The results were found to be attractive but at the cost of complicated numerical computation, thus limiting its application to a small PV systems. A MATLAB based modeling to study the effects of partial shading in a PV array was proposed in [25]. However, the work utilized the R_s -model. As stated earlier, the R_s -model exhibits serious deficiencies when subjected to high temperature variations. This can be very crucial when simulation of large PV array system is required. In [29], PSpice based modeling to study the effects of bypass diode configurations on PV modules was proposed. In this work, the authors used the conventional two-diode model with Bishop's model [30]. However, the model requires additional parameters to characterize the I - V and P - V curves, which in turn increases the computation burden.

In view on the importance of this issue, this paper proposes a practical modeling and simulation method, which can predict the I - V and P - V characteristics of large PV arrays. It can be used to study the effect of temperature and insolation variation, varying shading patterns, and the role of array configuration on the PV characteristics. The simulation is developed using the MATLAB environment. An important contribution of this work is the incorporation of the modified two-diode model as the main engine for the simulation. This model is known to have better accuracy, especially at low irradiance level. Despite its known advantages, previous researchers have avoided the use of the two-diode model, probably due to the significant increased in computational time. In this work, that problem is overcome by introducing an efficient computational method which requires only four parameters to characterize the I - V and P - V curves. In addition, the proposed work supports large array simulation that can be interfaced with MPPT algorithms and actual power electronic converters. The accurateness of the simulation model is compared with three modeling methods proposed by previous researchers, namely single-diode model [25], P&O [31], and Neural Network [32]. It is envisaged that the proposed work can be very useful for PV professionals who require simple, fast and accurate PV model to design their system.

2. PV model for partial shading

2.1. Two-diode model

The single-diode models [5–15] were based on the assumption that the recombination loss in the depletion region is absent. In a real solar cell, the recombination represents a substantial loss which cannot be adequately modeled using a single diode. Consideration of this loss leads to a more precise model known as the two-diode model [16]. However, the inclusion of the additional diode increases the parameters to seven (new parameters: I_{o2} , a_2).

The two-diode model is depicted in Fig. 1 [16]. Eq. (1) describes the output current of the cell:

$$I = I_{PV} - I_{D1} - I_{D2} - \left(\frac{V + IR_s}{R_p} \right) \quad (1)$$

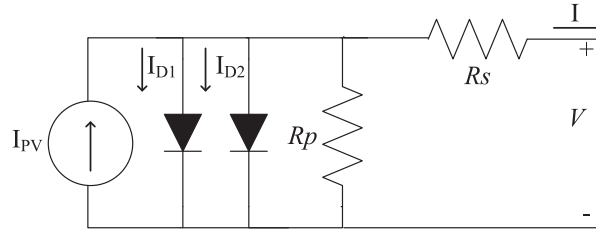


Fig. 1. Two-diode model.

where

$$I_{D1} = I_{o1} \left[\exp \left(\frac{V + IR_s}{a_1 V_{T1}} \right) - 1 \right], \quad I_{D2} = I_{o2} \left[\exp \left(\frac{V + IR_s}{a_2 V_{T2}} \right) - 1 \right] \quad (2)$$

where I_{PV} is the current generated by the incidence of light, I_{o1} and I_{o2} are the reverse saturation currents of diode 1 and diode 2, $V_{T1} (=a_1 \times N_s kT/q)$ and $V_{T2} (=a_2 \times N_s kT/q)$ are the thermal voltages having N_s cells connected in series, a_1 and a_2 represent the diode ideality constants, q is the electron charge ($1.60217646 \times 10^{-19}$ C), k is the Boltzmann constant ($1.3806503 \times 10^{-23}$ J/K), and T is the temperature of the p - n junction in K.

In this work, current of the PV cell is used as the input of partial shading modeling. Therefore, Eq. (1) need to be expressed in terms of cell output voltage as:

$$V = V_T \ln \left[\exp \left(-\frac{V + IR_s}{V_{T2}} \right) \left\{ \left(\frac{I_{PV} + I_{o1} + I_{o2} - I}{I_{o2}} \right) - \left(\frac{V + IR_s}{R_p I_{o2}} \right) \right\} - 1 \right] - IR_s \quad (3)$$

where

$$V_T = \frac{V_{T1} V_{T2}}{V_{T1} - V_{T2}} \quad (4)$$

Although greater accuracy can be achieved using this model, it requires the computation of seven parameters, namely I_{PV} , I_{o1} , I_{o2} , R_p , R_s , a_1 and a_2 . To simplify computation effort, several researchers assumed $a_1 = 1$ and $a_2 = 2$. The latter is an approximation of the Schokley–Read–Hall recombination in the space charge layer in the photodiode [16]. Although this assumption is widely used but not always true [33]. As discussed in the introduction section, many attempts have been made to reduce the computational time of this model. However they appear to be unsatisfactory.

2.2. Improved computational method

2.2.1. Simplification of saturation current equation

The equation for PV current as a function of temperature and irradiance can be written as

$$I_{PV} = (I_{PV_STC} + K_i \Delta T) \frac{G}{G_{STC}} \quad (5)$$

where I_{PV_STC} (in Ampere) is the light generated current at Standard Test Conditions (STC), $\Delta T = T - T_{STC}$ (in Kelvin, $T_{STC} = 25^\circ\text{C}$), G is the surface irradiance of the cell and G_{STC} (1000 W/m^2) is the irradiance at STC. The constant K_i is the short-circuit current coefficient, normally provided by the manufacturer. The well known diode saturation current equation is given:

$$I_0 = I_{0_STC} \left(\frac{T_{STC}}{T} \right)^3 \exp \left[\frac{qE_g}{ak} \left(\frac{1}{T_{STC}} - \frac{1}{T} \right) \right] \quad (6)$$

where E_g is the band gap energy of the semiconductor and I_{0_STC} is the nominal saturation current at STC. An improved equation to describe the saturation current which considers the temperature variation is given by [15]:

$$I_0 = \frac{(I_{sc_STC} + K_i \Delta T)}{\exp[(V_{oc_STC} + K_v \Delta T)/aV_T] - 1} \quad (7)$$

The constant K_v is the open circuit voltage coefficient. This value is available from the datasheet.

For the two-diode model, several researchers have calculated the values of I_{o1} and I_{o2} using iteration. The iteration approach greatly increases the computation time, primarily due to the non-suitable values of the initial conditions [34]. In general, I_{o2} is 3–7 orders of magnitude larger than I_{o1} . Furthermore, most of the previous works consider the ideality factors $a_1 = 1$ and $a_2 = 2$. In this work, we propose a modification of Eq. (7) and apply it to the two-diode model. No attempt has been made to this equation to solve for the saturation currents. To maintain the equation in the same form as in Eq. (7), both reverse saturation currents I_{o1} , I_{o2} are set to be equal in magnitude, i.e.

$$I_{o1} = I_{o2} = \frac{(I_{sc_STC} + K_I \Delta T)}{\exp[(V_{oc_STC} + K_V \Delta T)/\{(a_1 + a_2)/p\}V_T] - 1} \tag{8}$$

The equalization simplifies the computation as no iteration is required; the solution can be obtained analytically. Diode ideality factors a_1 and a_2 represent the diffusion and recombination current component, respectively. In accordance to Shockley’s diffusion theory, the diffusion current, a_1 must be unity [16]. The value of a_2 , however, is flexible. Based on extensive simulation carried out, it is found that if $a_2 \geq 1.2$, the best match between the proposed model and practical I – V curve is observed. Since $(a_1 + a_2)/p = 1$ and $a_1 = 1$, it follows that variable p can be chosen to be ≥ 2.2 . The following expression for I_{o1} , I_{o2} results:

$$I_{o1} = I_{o2} = \frac{(I_{sc_STC} + K_I \Delta T)}{\exp[(V_{oc_STC} + K_V \Delta T)/V_T] - 1} \tag{9}$$

This generalization can eliminate the ambiguity in selecting the values of a_1 and a_2 . Using Eqs. (5) and (8), five parameters of this model can be readily determined, i.e. I_{pv} , I_{o1} , I_{o2} , a_1 and a_2 .

2.2.2. Determination of R_p and R_s values

The remaining two parameters in Eq. (1), i.e. R_p and R_s are obtained through iteration. Several researchers have evaluated these two parameters independently, but the results are unsatisfactory. In this work, R_p and R_s are calculated simultaneously, similar to the procedure proposed in [15]. This approach has not been applied for two-diode model. The idea is maximum power point (P_{mp}) matching; i.e. to match the calculated peak power ($P_{mp,C}$) and the experimental (from manufacturer’s data-sheet) peak power ($P_{mp,E}$) by iteratively increasing the value of R_s while simultaneously calculating the R_p value. From Eq. (1) at maximum power point condition, the expression for R_p can be rearranged and rewritten as

$$R_p = \frac{V_{mp_STC} + I_{mp_STC} R_s}{\left\{ I_{pv} - I_{o1} \left[\exp \left(\frac{V_{mp_STC} + I_{mp_STC} R_s}{a_1 V_T} \right) - 1 \right] - I_{o2} \left[\exp \left(\frac{V_{mp_STC} + I_{mp_STC} R_s}{a_2 V_T} \right) - 1 \right] - \frac{P_{max,E}}{V_{mp_STC}} \right\}} \tag{10}$$

The initial conditions for both resistances are given below:

$$R_{s0} = 0; \quad R_{p0} = \frac{V_{mp_STC}}{I_{sc_STC} - I_{mp_STC}} - \frac{V_{oc_STC} - V_{mp_STC}}{I_{mp_STC}} \tag{11}$$

The initial value of R_p is the slope of the line segment between short-circuit and the maximum power points. For every iteration, the value of R_p is calculated simultaneously using Eq. (10). With the availability of all the seven parameters, the output current of the cell can now be determined using the standard Newton–Raphson method. The flowchart that describes the P_{mp} matching algorithm is given in Fig. 2.

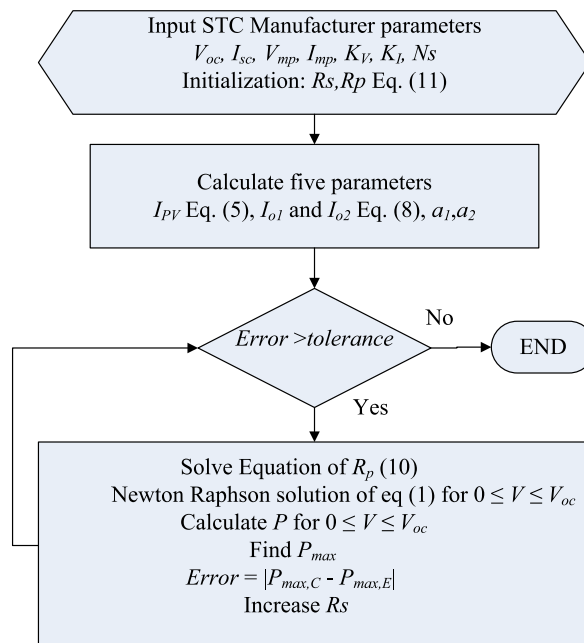


Fig. 2. Matching algorithm.

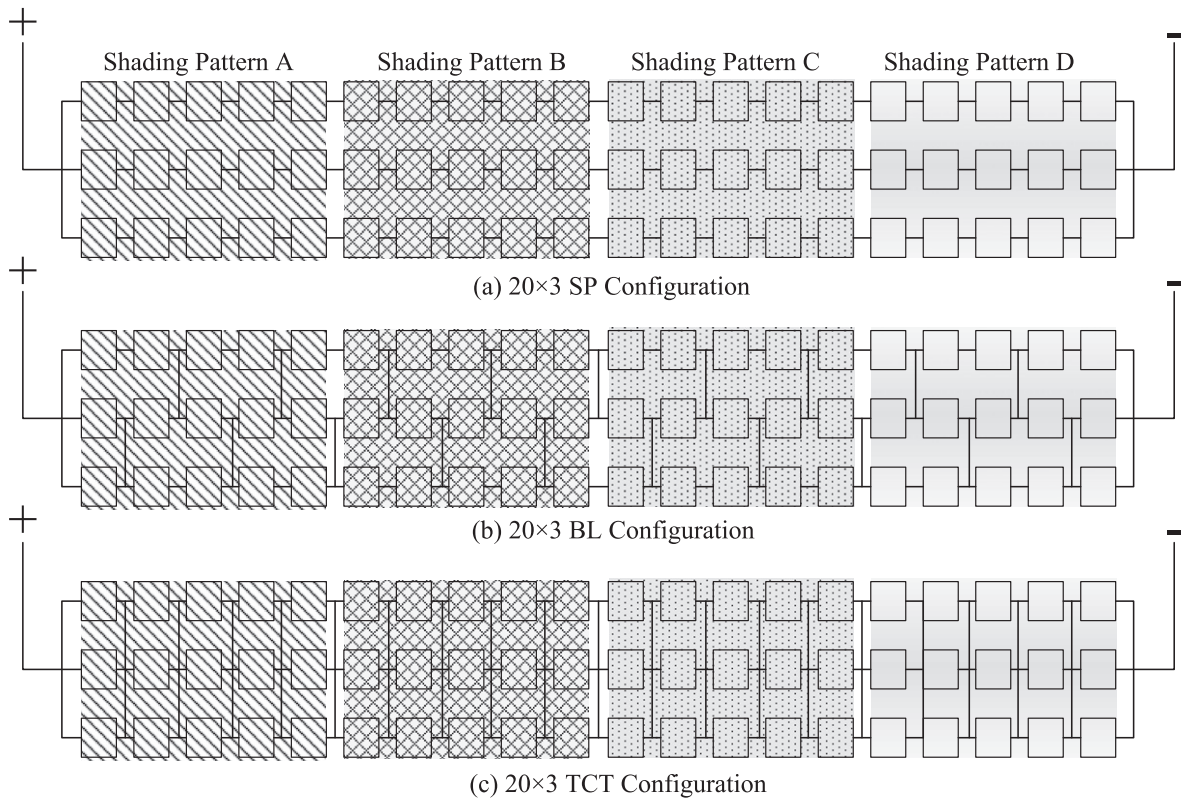


Fig. 3. SP, BL and TCT connections for 20 × 3 PV array.

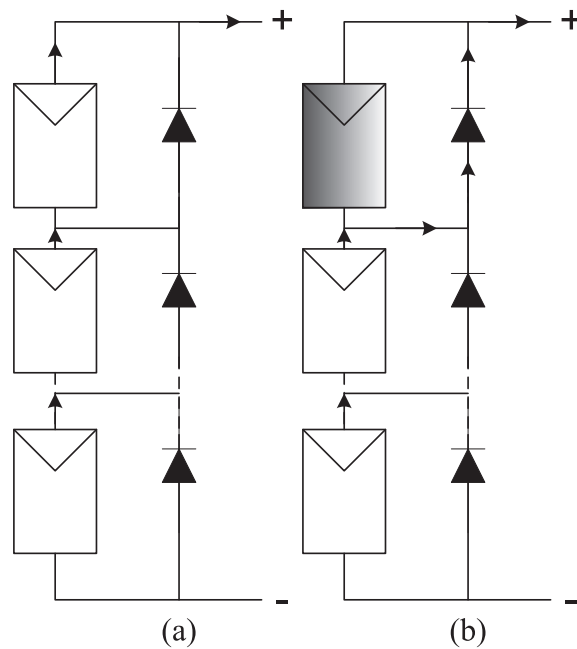


Fig. 4. (a) Module during normal conditions and (b) bypass operation during partial shading.

3. Partial shading modeling

A PV array is arrangement of several PV modules, connected in various interconnected topologies. Three types of interconnections structure are typically used namely, series–parallel (SP), bridge link (BL), and total cross tied (TCT). Fig. 3 depicts

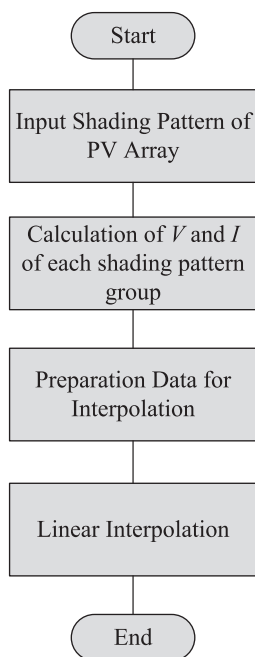


Fig. 5. Flow chart of partial shading modeling.

the aforementioned configurations for a 20×3 PV array. For simplicity, four types of shading patterns, labeled A–D are shown. For the series connected modules in SP configuration, due to the partial shading condition, the optimum operating point (M_{pp}) is being forced to move from the non-shaded to the shaded module [35]. However, for the BL and TCT interconnections, due to the additional wires in the modules connections, new current paths are created and the PV output power can be increased under the non-uniform insolation conditions. This kind of connections can be useful under certain shading patterns [36].

The characteristics of PV modules under shading conditions with bypass diodes connected at module terminal are explained as follows. In normal condition, i.e. when modules are not shaded, the bypass diodes are reversed biased. The current flows through each module, as shown in Fig. 4a. Under partially shaded conditions, the shaded cells behave as a load instead of generator and create the hot spot problem. The hot spot effect can be avoided by driving the current away from the non-shaded cells through a bypass diode as shown in Fig. 4b. In the shaded area, the bypass diode is in forward biased; therefore it conducts the current produced by the non-shaded part. Since the shaded modules are bypassed, multiple peaks in the I – V and P – V characteristics curves are created.

For a large PV array, the ability of the simulation tool to resolve partial shading problem is very crucial. This is due to the fact that in large array configuration, the likelihood for partial shading to occur is large. The flow chart in Fig. 5 shows the procedure to compute the I – V and P – V curves for any array size during partial shading. For simplicity, only SP configuration is modeled. Once the shading pattern and temperature of the modules are generated, a software routine will be executed which will carry out the following tasks: (1) determination of shading patterns and temperature for a particular shading group, (2) calculation of voltage and current for each group based on the two-diode model, subjected to a known shading pattern and (3) performing linear interpolation with extrapolation techniques to form the continuous I – V and P – V curves.

4. Results and discussion

4.1. Verification of two-diode model

The two-diode model described in this paper is validated by measured parameters of selected PV modules. The specifications of these modules are summarized in Table 1. The computational results are compared with the R_s [6] and R_p [11] models.

Table 2 shows the parameters for the proposed two-diode model. Although the model has more variables, the actual number of parameters computed are only four because $I_{o1} = I_{o2}$ while a_1 and a_2 can be chosen arbitrarily from (8).

For brevity only MSX-60 [37] and KC200GT [38] will be used in the model verification. The SM55 [39] will be included in the validation of partial shading modeling. Fig. 6 shows the I – V curves for a single KC200GT module for different levels of irradiation (per unit quantity: Sun = 1 equivalent to 1000 W/m^2). The calculated values from the proposed two-diode and

Table 1
STC specifications for the three modules used in the experiments.

Parameter	BP Solar MSX-60	Kyocera KG200GT	Siemens SM55
I_{sc}	3.8 A	8.21 A	3.45 A
V_{oc}	21.1 V	32.9 V	21.7 V
I_{mp}	3.5 A	7.61 A	3.15 A
V_{mp}	17.1 V	26.3 V	17.4 V
K_v	-80 mV/°C	-123 mV/°C	-77 mV/°C
K_i	3 mA/°C	3.18 mA/°C	1.2 mA/°C
N_s	36	54	36

Table 2
Parameters for the proposed two-diode model.

Parameter	BP Solar MSX-60	Kyocera KG200GT	Siemens SM55
I_{sc}	3.8 A	8.21 A	3.45 A
V_{oc}	21.1 V	32.9 V	21.7 V
I_{mp}	3.5 A	7.61 A	3.15 A
V_{mp}	17.1 V	26.3 V	17.4 V
$I_{o1} = I_{o2}$	4.704×10^{-10} A	4.218×10^{-10} A	2.232×10^{-10} A
I_{PV}	3.80 A	8.21 A	3.45 A
R_p	176.4 Ω	160.5 Ω	144.3 Ω
R_s	0.35 Ω	0.32 Ω	0.47 Ω

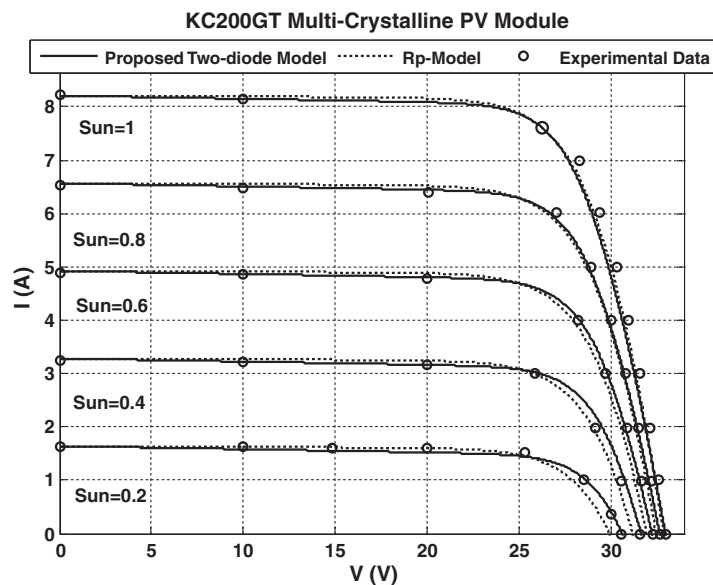


Fig. 6. I - V curves of R_p -model and proposed two-diode model of the KC200GT PV module for several Irradiation levels.

R_p -models are evaluated against measured data from the manufacturer’s datasheet. Comparison to the R_s -model is not included to avoid overcrowding of plot. However, the results for the R_s -model will be analyzed later in the performance evaluation between the three models.

The proposed two-diode model and the R_p -model exhibit similar results at STC. This is expected because both models use the similar maximum power matching algorithm to evaluate the model parameters at STC. However, as irradiance goes lower, more accurate results are obtained from the two-diode model, especially in the vicinity of the open circuit voltage. At V_{oc} , the R_p -model shows departure from the experimental data, suggesting that R_p -model is inadequate when dealing with low irradiance level. This is envisaged to have significant implication during partial shading.

The performance of the models when subjected to temperature variation is considered next. All measurements are conducted at STC irradiance of 1000 W/m^2 . The proposed model is compared to the R_s -model. The comparison specifically is chosen to highlight the significant problems with the R_s -model when subjected to temperature variations. The R_p -model is not shown for simplicity, but will be included later in the analysis that compares all the three models together. Two modules are

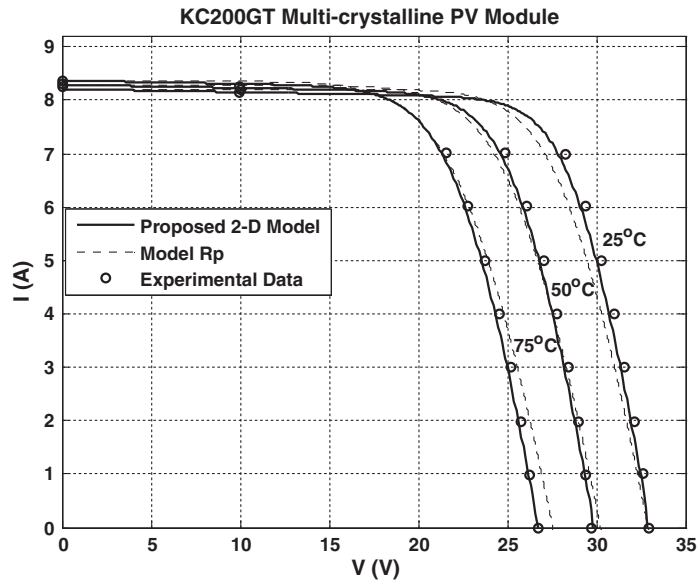


Fig. 7. I - V curves of R_s and proposed two-diode model of the KC200GT PV module for several temperature levels.

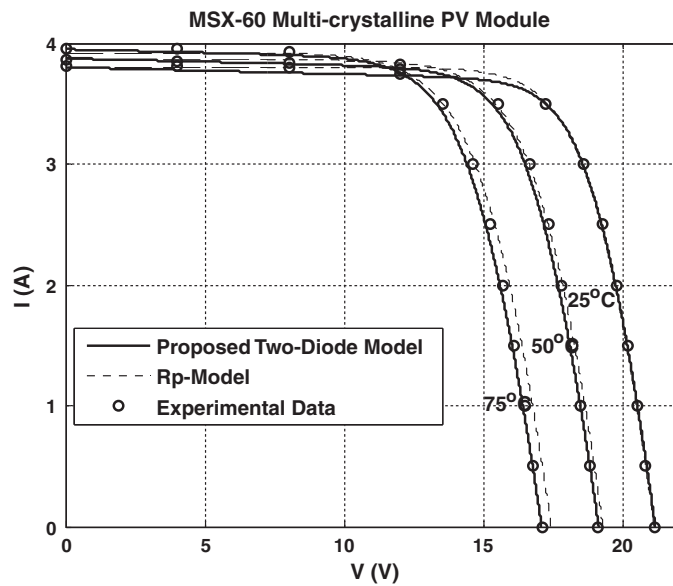


Fig. 8. I - V curves of R_s and proposed two-diode model of the MSX 60 PV module for several temperature levels @ 1 kW/m^2 .

tested, namely the KC200GT and MSX-60. As can be seen in Figs. 7 and 8, respectively, the curves I - V computed by the two-diode model fit accurately to the experimental data for all temperature conditions. In contrast, at higher temperature, results from the R_s -model deviates from the measured values quite significantly.

Fig. 9a shows the absolute error of the all the three modeling methods with respect to the experimental data. The proposed model is compared to the single-diode model with R_s [6] and R_p [15], respectively. The absolute errors are evaluated at irradiance of 200 W/m^2 . For clarity, the errors are plotted on the same graphs. As can be seen, for the whole range of experimental data, the proposed model is superior, especially at the vicinities of the open circuit voltage. Fig. 9b analyzes the three modeling methods with respect the temperature changes. It can be observed that R_s -model yields inaccurate results particularly at the neighborhood of the open circuit voltage. This is to be expected as this model does not account for the open circuit voltage coefficient, K_V [6]. The proposed and R_p -models offers an almost equivalent performance for the whole range of temperature variations.

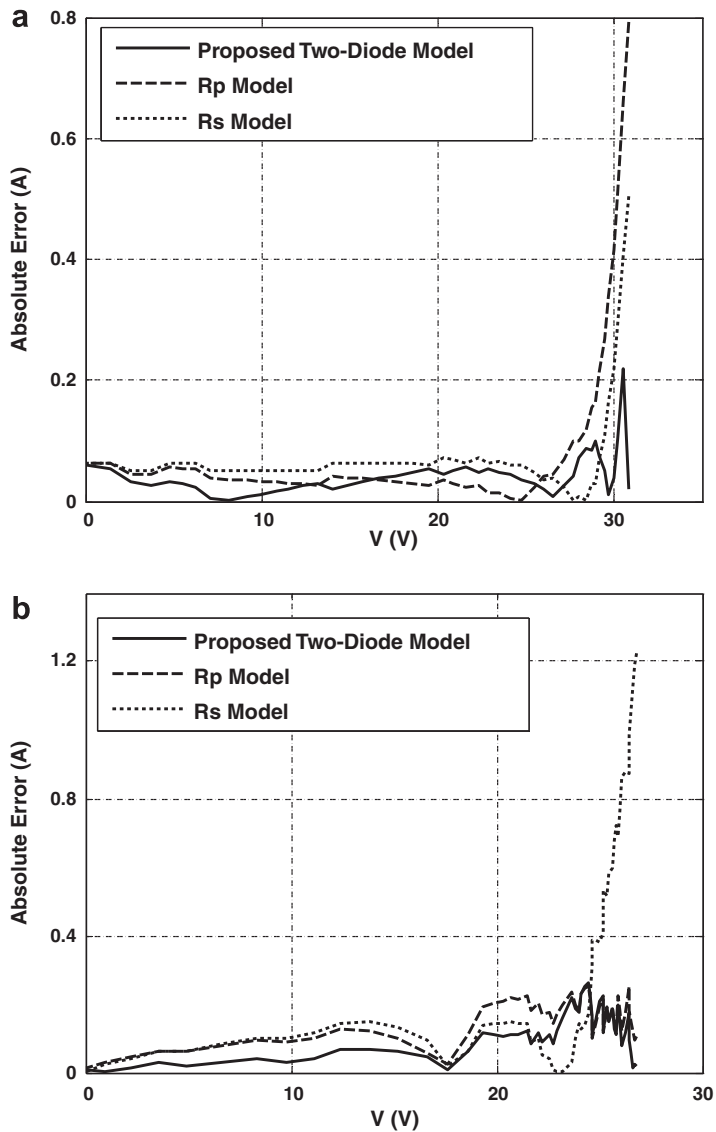


Fig. 9. Absolute errors for proposed two-diode model, R_p - and R_s -models. (a) For KC200GT PV module and (b) for MSX-60 PV module.

Table 3

Shading pattern of the array used in illustration.

Curves	Shading pattern A (kW/m ²)	Shading pattern B (kW/m ²)	Shading pattern C (kW/m ²)	Shading pattern D (kW/m ²)
a	1	0.75	0.5	0.25
b	0.9	0.75	0.5	0.1
c	0.75	0.5	0.25	0.1
d	0.8	0.6	0.4	0.2

The extensive experimental verification above has proven that the two-diode model is superior that the single-diode model with R_s and R_p . This justifies its usage in a more complicated situation such as partial shading.

4.2. Validation of modeling for partial shading

In order to verify the accurateness of the proposed model for partial shading conditions, the result is compared with the work carried out in [32]. The latter is based on Artificial Neural Network. In [32], a real-time PV emulator was designed to emulate P - V characteristics curves with a special focus on partial shading conditions. For the PV modules model, the P - V

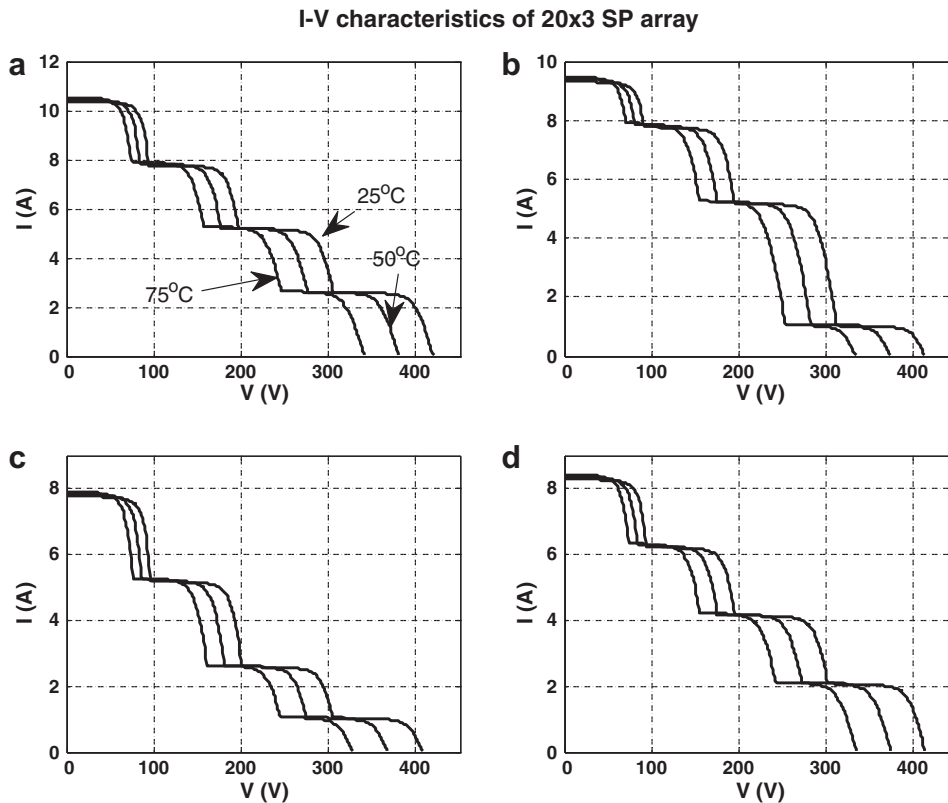


Fig. 10. *I-V* characteristics curves for Table 3.

characteristic was generated based on Sandia's PV model. The main component of the developed emulator consists of two personal computers (PCs) with Analog–Digital (AD) and Digital–Analog (DA) hardware under a real-time dSPACE platform. Several inhomogeneous irradiance distributions were used to investigate the behavior of the proposed system.

For simplicity, only 20×3 SP configuration is discussed here. However, it can be increased for any number $M \times N$ array, where M and N represent the number of series and parallel modules, respectively. Four shading patterns are considered; they are depicted in Table 3. For every curve, the evaluation is done at three different temperatures, i.e. 25 °C, 50 °C, and 75 °C. Figs. 10 and 11 show the *I-V* and *P-V* characteristics curves for the shading patterns described above. It is expected that the curves exhibit multiple number of peaks that are equal to the number of irradiance levels imposed on the array. However, more precisely, it depends on the temperature of the modules, the insolation level, the shading pattern, and the array configuration [25].

In order to verify the accurateness of the proposed modeling approach comparison is made with 10 shading patterns. The results are shown in Tables 4–6 for temperatures at 25°, 50° and 75°, respectively. It can be seen that values obtained for $V_{mp,G}$ and $P_{mp,G}$ (global peak values) are in close agreement with the results [32]. Fig. 12 shows the relative error of $P_{mp,G}$ for the proposed and single-diode model. It can be observed that, in general, the proposed method gives comparable $P_{mp,G}$ errors to the single-diode method (less than 5%, except for a few cases).

4.3. Simulation with converter and controller

Another important aspect of the PV simulation model is the ability to interface with the power electronic converters. Fig. 13 depicts a simulation example of a PV system, in which a boost-type dc–dc converter (with MPPT controller) is included. The SM55 PV modules are used in the simulation for a 20×3 array configuration. The MPPT controller utilizes the conventional Perturbation and Observe (P&O) algorithm to track the MPP. The performance of P&O is tested for shading pattern of curve (a) of Fig. 11 at 25°C. The simulation results are shown in Fig. 14.

Initially the array receives a uniform irradiation of ($G = 1 \text{ kW/m}^2$). It is observed that, prior to the shading occurrence, i.e. at $t = 0.5 \text{ s}$, the array's voltage and current are retained at 350 V and 9.44 A, respectively. This corresponds to the maximum power point, i.e. 3220 W. Due to the shading conditions (at $t = 0.5 \text{ s}$), operating point is shifted to a new minima at 820 W. This clearly highlights the limitation of the P&O scheme when multiple peaks are present. It cannot distinguish between the global and local maxima.

P-V characteristics of an array

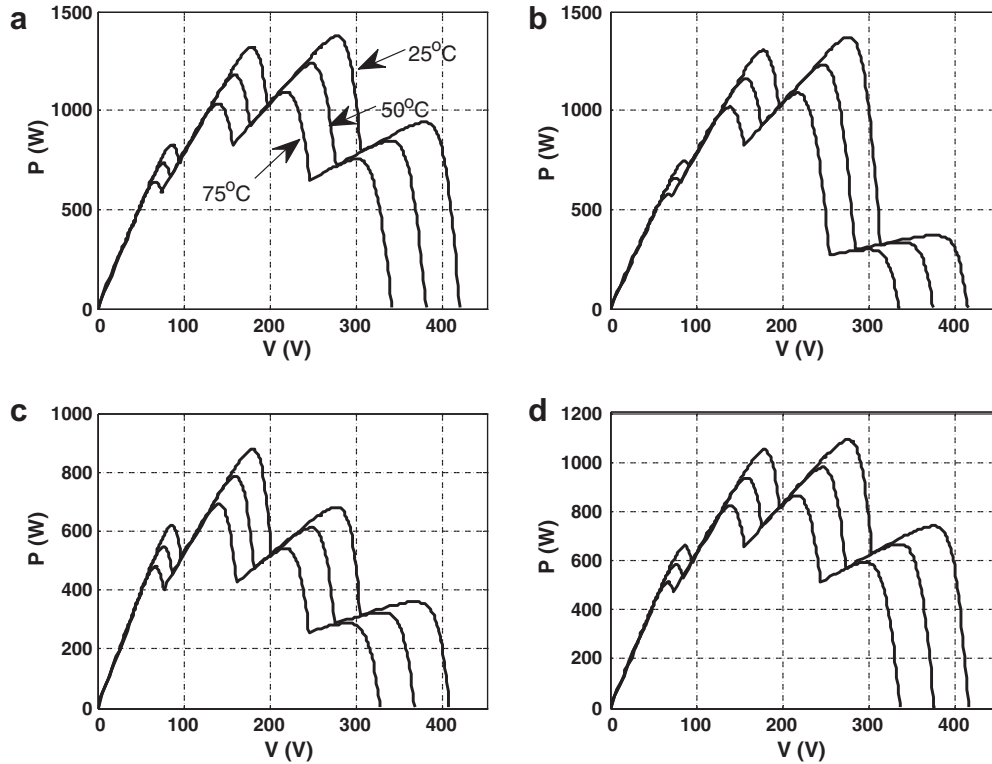


Fig. 11. P–V characteristics curves for Table 3.

Table 4

The V_{dc} and P_{dc} outputs of 20×3 PV array under partially shaded conditions at 25 °C.

Time	Shading pattern 1 = (1000 W/m ²)				P&O [31]		ANN [32]		Single-diode model [25]		Proposed modeling	
	A	B	C	D	V_{dc}	P_{dc}	V_{dc}	P_{dc}	V_{dc}	P_{dc}	V_{dc}	P_{dc}
1	1	0.75	0.5	0.25	384.72	971.44	276.38	1383.1	271	1350.8	275	1359.6
2	0.75	0.25	0.25	0.1	373.67	377.78	263.12	646.13	247	595.76	263	620.9
3	1	0.5	0.3	0.1	382.51	387.11	174.67	866.76	178	872.02	180	883.4
4	0.8	0.6	0.4	0.2	380.3	770.38	274.17	1100	265	1058.9	272	1077.9
5	0.9	0.6	0.3	0.1	382.51	387.7	172.46	1020.6	176	1030.7	178	1047.7
6	0.6	0.5	0.4	0.3	369.25	1117.4	369.25	1117.4	345	1046.4	360	1076.8
7	0.75	0.5	0.2	0.1	375.88	381.06	172.46	847.77	172	844.17	177	867.6
8	1	0.6	0.3	0.15	382.51	580.18	174.67	1030.4	177	1044.5	179	1055.2
9	1	1	0.5	0.25	386.93	977.16	165.83	1566.3	173	1621.4	171	1632.4
10	1	0.5	0.5	0.2	382.51	774.62	267.54	1301.6	259	1247.1	266	1282.4

Table 5

The V_{dc} and P_{dc} outputs of 20×3 PV array under partially shaded conditions at 50 °C.

Time	Shading pattern 1 = (1000 W/m ²)				P&O [31]		ANN [32]		Single-diode model [25]		Proposed modeling	
	A	B	C	D	V_{dc}	P_{dc}	V_{dc}	P_{dc}	V_{dc}	P_{dc}	V_{dc}	P_{dc}
1	1	0.75	0.5	0.25	338.29	856.99	241.01	1213.4	240	1206	244	1220.2
2	0.75	0.25	0.25	0.1	325.03	329.46	229.95	560.97	217	520.76	231	553.01
3	1	0.5	0.3	0.1	336.08	339.24	152.56	755.81	158	775.9	161	790.67
4	0.8	0.6	0.4	0.2	336.08	677.21	241.01	964.26	236	940.89	243	965.92
5	0.9	0.6	0.3	0.1	336.08	339.93	150.35	885.98	156	914.9	158	935.20
6	0.6	0.5	0.4	0.3	322.81	979.39	322.81	979.39	307	925.6	323	964.16
7	0.75	0.5	0.2	0.1	329.45	333.01	150.35	735.27	153	746.31	158	774.04
8	1	0.6	0.3	0.15	336.08	509.23	150.35	895.62	159	929.17	160	943.68
9	1	1	0.5	0.25	340.5	863.12	143.72	1351.1	155	1435.9	152	1446.9
10	1	0.5	0.5	0.2	336.08	681.71	232.16	1136.5	229	1101.9	235	1143.5

Table 6
The V_{dc} and P_{dc} outputs of 20×3 PV array under partially shaded conditions at 75 °C.

Time	Shading pattern 1 = (1000 W/m ²)				P&O [31]		ANN [32]		R _s -model [25]		Proposed modeling	
	A	B	C	V _{dc}	V _{dc}	P _{dc}	V _{dc}	P _{dc}	V _{dc}	P _{dc}	V _{dc}	P _{dc}
1	1	0.75	0.5	0.25	338.29	856.99	241.01	1213.4	240	1206	244	1220.2
2	0.75	0.25	0.25	0.1	325.03	329.46	229.95	560.97	217	520.76	231	553.01
3	1	0.5	0.3	0.1	336.08	339.24	152.56	755.81	158	775.9	161	790.67
4	0.8	0.6	0.4	0.2	336.08	677.21	241.01	964.26	236	940.89	243	965.92
5	0.9	0.6	0.3	0.1	336.08	339.93	150.35	885.98	156	914.9	158	935.20
6	0.6	0.5	0.4	0.3	322.81	979.39	322.81	979.39	307	925.6	323	964.16
7	0.75	0.5	0.2	0.1	329.45	333.01	150.35	735.27	153	746.31	158	774.04
8	1	0.6	0.3	0.15	336.08	509.23	150.35	895.62	159	929.17	160	943.68
9	1	1	0.5	0.25	340.5	863.12	143.72	1351.1	155	1435.9	152	1446.9
10	1	0.5	0.5	0.2	336.08	681.71	232.16	1136.5	229	1101.9	235	1143.5

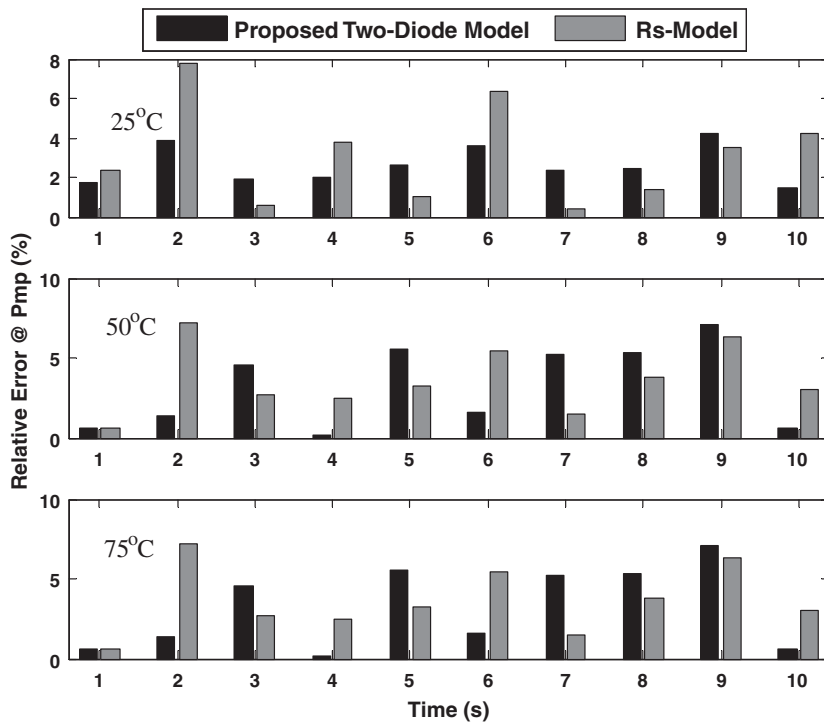


Fig. 12. Relative error of P_{mp} for proposed and R_s models for Tables 4–6.

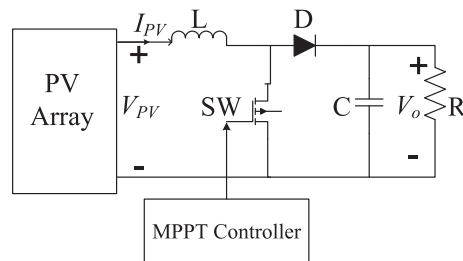


Fig. 13. PV system description utilizing proposed model.

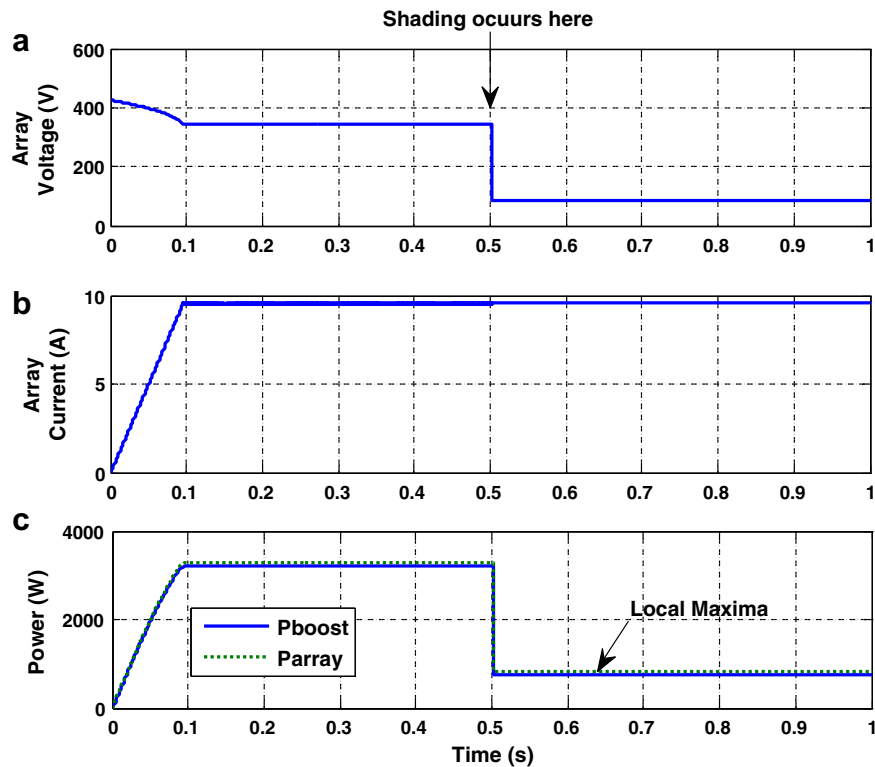


Fig. 14. (a–c) Output voltage, current, and output power from the PV array.

5. Conclusion

In this paper, a partial shading modeling based on an improved two-diode model is proposed. The proposed modeling supports large array simulation that can be interfaced with MPPT algorithms and actual power electronic converters. It is observed that the two-diode model is superior to the R_p - and R_s -models. The accurateness of the partial shading modeling is compared with the three types of modeling methods. Furthermore a PV system, together with the power converters and controllers are simulated. The results are found to be in close agreement with theoretical prediction.

Acknowledgments

The authors would like to thank Universiti Teknologi Malaysia for providing the facilities and research grant to conduct this research and the reviewers for their valuable comments.

References

- [1] M.C. Glass, Improved solar array power point model with SPICE realization, in: Proc. 31st Intersoc. Energy Convers. Eng. Conf. (IECEC), vol. 1, 1996, pp. 286–291.
- [2] Y.T. Tan, D.S. Kirschen, N. Jenkins, A model of PV generation suitable for stability analysis, IEEE Trans. Energy Convers. 19 (4) (2004) 748–755.
- [3] A. Kajihara, A.T. Harakawa, Model of photovoltaic cell circuits under partial shading, in: Proc. IEEE Int. Conf. Ind. Technol. (ICIT), 2005, pp. 866–870.
- [4] N.D. Benavides, P.L. Chapman, Modeling the effect of voltage ripple on the power output of photovoltaic modules, IEEE Trans. Ind. Electron. 55 (7) (2008) 2638–2643.
- [5] W. Xiao, W.G. Dunford, A. Capel, A novel modeling method for photovoltaic cells, in: Proc. IEEE 35th Annu. Power Electron. Spec. Conf. (PESC), vol. 3, 2004, pp. 1950–1956.
- [6] G. Walker, Evaluating MPPT converter topologies using a matlab PV model, J. Elect. Electron. Eng., Aust. 21 (1) (2001) 45–55.
- [7] F. González-Longatt, Model of Photovoltaic Module in Matlab™, II CIBELEC, 2005.
- [8] N. Celik, N. Acikgoz, Modelling and experimental verification of the operating current of mono-crystalline photovoltaic modules using four- and five-parameter models, Appl. Energy 84 (1) (2007) 1–15.
- [9] Y.C. Kuo, T.-J. Liang, J.-F. Chen, Novel maximum-power-point tracking controller for photovoltaic energy conversion system, IEEE Trans. Ind. Electron. 48 (3) (2001) 594–601.
- [10] Y. Yusof, S.H. Sayuti, M. Abdul Latif, M.Z.C. Wanik, Modeling and simulation of maximum power point tracker for photovoltaic system, in: Proc. Nat. Power Energy Conf. (PEC), 2004, pp. 88–93.
- [11] C. Carrero, J. Amador, S. Arnaltes, A single procedure for helping PV designers to select silicon PV module and evaluate the loss resistances, Renew. Energy 32 (15) (2007) 2579–2589.
- [12] S. Liu, R.A. Dougal, Dynamic multiphysics model for solar array, IEEE Trans. Energy Convers. 17 (2) (2002) 285–294.

- [13] S. Yadir, M. Benhmida, M. Sidki, E. Assaid, M. Khaidar, New method for extracting the model physical parameters of solar cell using explicit analytic solutions of current–voltage equation, in: Proc. Int. Conf. Microelectronics (ICM), 2009, pp. 390–393.
- [14] S. Aazou, E.M. Assaid, Modeling real photovoltaic solar cell using Maple, in: Proc. Int. Conf. Microelectronics (ICM), 2009, pp. 394–397.
- [15] M.G. Villalva, J.R. Gazoli, E.R. Filho, Comprehensive approach to modeling and simulation of photovoltaic arrays, *IEEE Trans. Power Electron.* 24 (5) (2009) 1198–1208.
- [16] C. Sah, R.N. Noyce, W. Shockley, Carrier generation and recombination in p-n junctions and p-n junction characteristics, *Proc. IRE* 45 (9) (1957) 1228–1243.
- [17] A. Gow, C.D. Manning, Development of a photovoltaic array model for use in power–electronics simulation studies, *IEE Proc. Elect. Power Appl.* 146 (2) (1999) 193–200.
- [18] J.A. Gow, C.D. Manning, Development of a model for photovoltaic arrays suitable for use in simulation studies of solar energy conversion systems, in: Proc. 6th Int. Conf. Power Electron. Variable Speed Drives, 1996, pp. 69–74.
- [19] S. Chowdhury, G.A. Taylor, S.P. Chowdhury, A.K. Saha, Y.H. Song, Modelling, simulation and performance analysis of a PV array in an embedded environment, in: Proc. 42nd Int. Univ. Power Eng. Conf. (UPEC), 2007, pp. 781–785.
- [20] A. Hovinen, Fitting of the solar cell/V–curve to the two diode model, *Phys. Scripta T54* (1994) 175–176.
- [21] J. Hyvarinen, J. Karila, New analysis method for crystalline silicon cells, in: Proc. 3rd World Conf. Photovoltaic Energy Convers., vol. 2, 2003, pp. 1521–1524.
- [22] K. Kurobe, H. Matsunami, New two–diode model for detailed analysis of multicrystalline silicon solar cells, *Jpn. J. Appl. Phys.* 44 (2005) 8314–8321.
- [23] K. Nishioka, N. Sakitani, K. Kurobe, Y. Yamamoto, Y. Ishikawa, Y. Uraoka, T. Fuyuki, Analysis of the temperature characteristics in polycrystalline Si solar cells using modified equivalent circuit model, *Jpn. J. Appl. Phys.* 42 (2003) 7175–7179.
- [24] K. Nishioka, N. Sakitani, Y. Uraoka, T. Fuyuki, Analysis of multicrystalline silicon solar cells by modified 3–diode equivalent circuit model taking leakage current through periphery into consideration, *Solar Energy Mater. Solar Cells* 91 (13) (2007) 1222–1227.
- [25] H. Patel, V. Agarwal, MATLAB-based modeling to study the effects of partial shading on PV array characteristics, *IEEE Trans. Energy Convers.* 23 (1) (2008) 302–310.
- [26] M.C. Alonso-Gracia, J.M. Ruiz, F. Chenlo, Experimental study of mismatch and shading effects in the I–V characteristic of a photovoltaic module, *Solar Energy Mater. Solar Cells* 90 (3) (2006) 329–340.
- [27] H. Kawamura, K. Naka, N. Yonekura, S. Yamanaka, H. Kawamura, H. Ohno, K. Naito, Simulation of I–V characteristics of a PV module with shaded PV cells, *Solar Energy Mater. Solar Cells* 75 (3/4) (2003) 613–621.
- [28] V. Quaschnig, R. Hanitsch, Numerical simulation of current–voltage characteristics of photovoltaic systems with shaded solar cells, *Solar Energy* 56 (6) (1996) 513–520.
- [29] S. Silvestre, A. Boronat, A. Chouder, Study of bypass diodes configuration on PV modules, *Appl. Energy* 86 (2009) 1632–1640.
- [30] J.W. Bishop, Computer simulation of the effects of electrical mismatches in photovoltaic cell interconnection circuits, *Solar Cells* 25 (1998) 73–89.
- [31] T. ESRAM, P.L. Chapman, Comparison of photovoltaic array maximum power point tracking techniques, *IEEE Trans. Energy Convers.* 22 (2007) 439–449.
- [32] Syafaruddin, E. Karatepe, T. Hiyama, Development of Real-Time Simulator based on Intelligent Techniques for Maximum Power Point Controller of PV Modules, *The International Journal of Innovative Computing, Information and Control (IJICIC)*, vol. 6, 2010, pp. 1623–1642.
- [33] K.R. McIntosh, P.P. Altermatt, G. Heiser, Depletion-region recombination in silicon solar cells: when does $mDR=2$? in: Proceedings of the 16th European Photovoltaic Solar Energy Conference, 2000, pp. 251–254.
- [34] N. Enebish, D. Agchbayar, S. Dorjkhand, D. Baatar, I. Ylemj, Numerical analysis of solar cell current–voltage characteristics, *Solar Energy Mater. Solar Cells* 29 (1993) 201–208.
- [35] E. Karatepe, T. Hiyama, M. Boztepe, M. Colak, Voltage based power compensation system for photovoltaic generation system under partially shaded insolation conditions, *Energy Convers. Manage.* 49 (2008) 2307–2316.
- [36] E. Karatepe, M. Boztepe, M. Colak, Development of a suitable model for characterizing photovoltaic arrays with shaded solar cells, *Solar Energy* 81 (2007) 977–992.
- [37] Solarex MSX60 and MSX64 Solar Arrays Datasheet, 1997. <<http://www.californiasolarcenter.org/newssh/pdfs/solarex-MSX64.pdf>>.
- [38] KC200GT High Efficiency Multicrystal Photovoltaic Module Datasheet Kyocera. <<http://www.kyocera.com.sg/products/solar/pdf/kc200gt.pdf>>.
- [39] Siemens Solar Module SM55. <<http://www.solarquest.com/microsolar/suppliers/siemens/sm55.pdf>>.